Table S1. Comparison of dust intensive optical properties – the lidar ratio (LR, in sr), particle linear depolarization ratio (PLDR), extinction Angstrom exponent over 355 to 532 nm ($EAE_{355-532}$), backscattering Angstrom exponent over 355 to 532 nm ($BAE_{355-532}$), extracted from literatures and simulated with the scattering models for the aerosol models defined in Table 1. "Sphd" and "Sph" refer to the Spheroid and Sphere models, respectively. The ranges of the simulations result from the variation of the CRI and those of the measurements represent the measurement errors provided by the literatures. The Floutsi-23 combines the results of Saharan, Central Asian and Middle Eastern dust reported by Floutsi et al. (2023); the Haarig-22 corresponds to a pure dust case reported by Haarig et al. (2022); and the Hu-20 corresponds to the pure dust layer of the "Case 3" in Hu et al. (2020).

VSD type	Scat. model	LR_{355}	LR_{532}	LR_{1064}	$PLDR_{355}$	$PLDR_{532}$	$PLDR_{1064}$	$EAE_{355-532}$	$BAE_{355-532}$
TD	IH	77±48	66±34	72±32	0.39±0.03	0.36±0.03	0.26±0.05	–0.06±0.05	–0.2±0.5
	Sphd	67±41	58±32	77±32	0.30±0.06	0.31±0.05	0.27±0.01	–0.18±0.03	–0.4±0.6
	Sph	30±25	27±32	36±25	0	0	0	–0.22±0.01	–0.2±0.7
FD	IH	91±61	58±29	50±23	0.42±0.07	0.43±0.03	0.37±0.02	–0.07±0.01	–0.7±0.9
	Sphd	91±58	55±29	57±25	0.26±0.06	0.29±0.06	0.31±0.05	–0.14±0.02	–1.2±0.7
	Sph	37±31	21±16	20±15	0	0	0	–0.13±0.02	–1.1±1.0
BD	IH	83±42	55±23	47±20	0.27±0.07	0.30±0.04	0.32±0.02	0.62±0.10	–0.2±0.5
	Sphd	86±39	52±21	53±22	0.18±0.04	0.21±0.05	0.27±0.04	0.67±0.13	–0.5±0.3
	Sph	44±30	24±15	20±14	0	0	0	0.76±0.12	–0.7±0.7
Measurements		**LR_{355}**	**LR_{532}**	**LR_{1064}**	**$PLDR_{355}$**	**$PLDR_{532}$**	**$PLDR_{1064}$**	**$EAE_{355-532}$**	**$BAE_{355-532}$**
Floutsi-23		47±14	47±14	–	0.24±0.03	0.30±0.03	–	0.10±0.20	0.2±0.1
Haarig-22		47±8	50±5	69±14	0.24±0.02	0.30±0.02	0.21±0.01	–0.01±0.19	0.04±0.5
Hu-20		51±8	45±7	–	0.32±0.07	0.34±0.05	0.31±0.04	0.02±0.30	–0.3±0.3

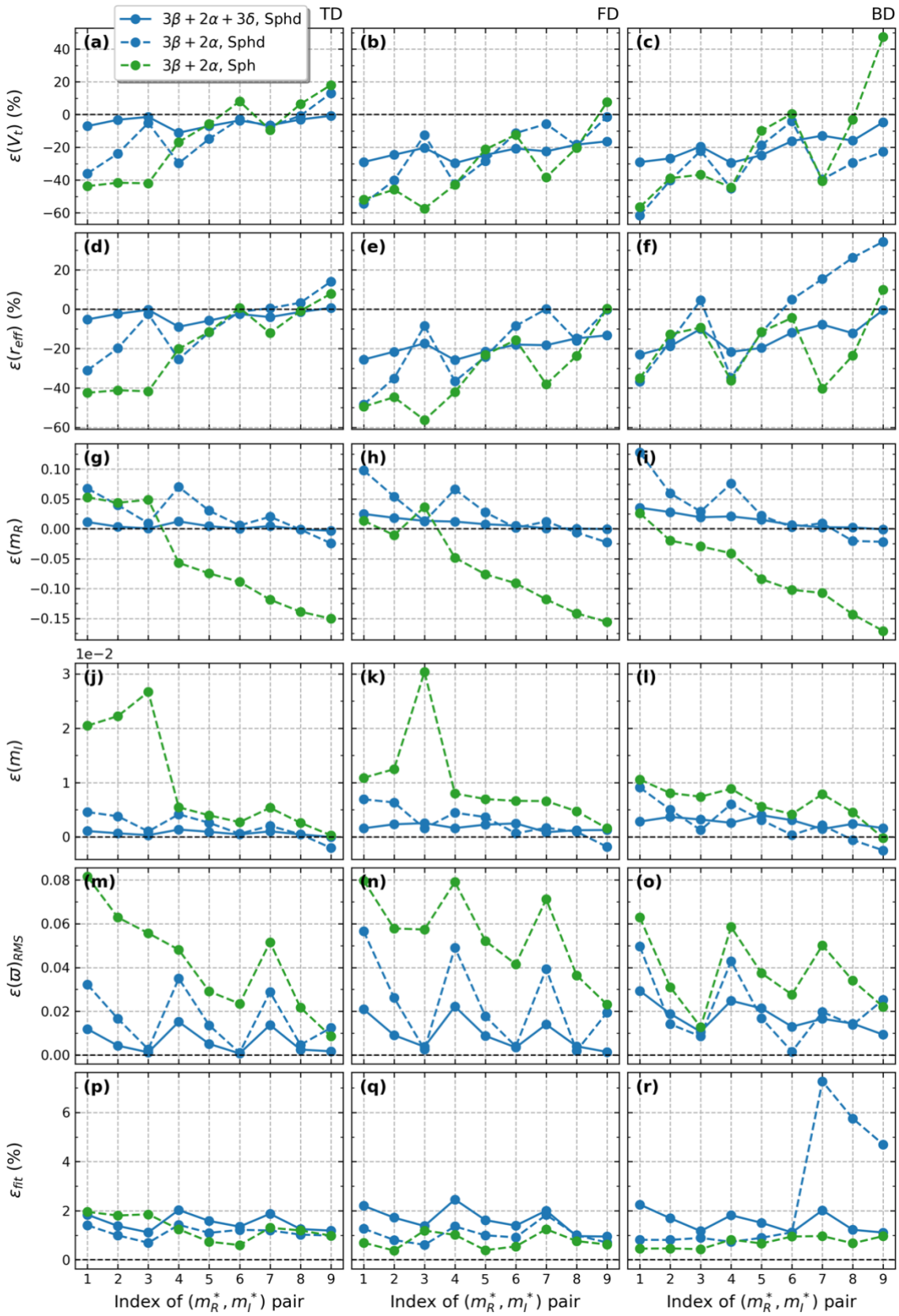

Figure S1. Same as Fig. 10 except that the optical datasets are generated by the Spheroid model and the retrieval configurations ($3\beta + 2\alpha + 3\delta$, Spheroid), ($3\beta + 2\alpha$, Spheroid), and ($3\beta + 2\alpha$, Sphere) are used

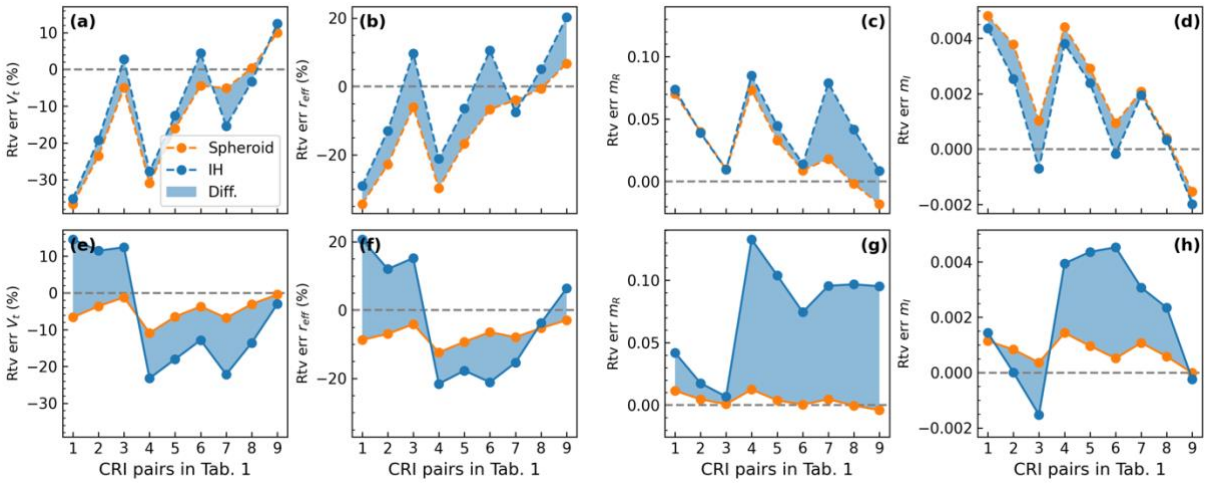

Figure S2. Same as Fig. 12 except that the optical datasets are generated by the Spheroid model.

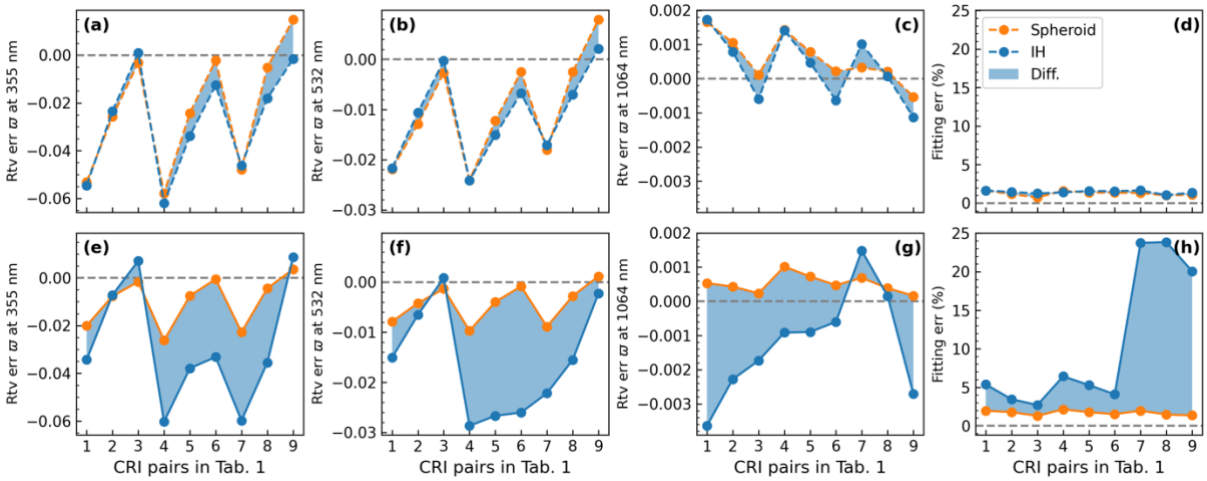

Figure S3. Same as Fig. 13 except that the optical datasets are generated by the Spheroid model.